J Therm Anal Calorim (2010) 99:495–500
DOI 10.1007/s10973-009-0165-6

In-plane thermal conductance measurement of one-dimensional nanostructures

Hsiao-Fang Lee · Benedict A. Samuel · M. A. Haque

Received: 19 February 2009 / Accepted: 16 April 2009 / Published online: 19 June 2009

Abstract We present a new analytical model for thermal conductivity measurement of one-dimensional nanostructures on substrates. The model expands the capability of the conventional 3ω technique, to make it versatile with both in and out of plane thermal conductivity measurement on specimens either freestanding or attached to substrates. We demonstrate the model on both conducting (aluminum) and semi-conducting (focused ion beam deposited platinum) specimens. The agreement with the established values in the literature suggests the superiority of this technique in terms of convenience and robustness of measurement.

Keywords 3ω technique · Thermal conductivity · FIB Pt nanowire

Introduction

Electrical and thermal transport properties of nanostructures exhibit significant size effects attributed to the increased surface-to-volume ratio and stronger influence of grain boundary scattering processes. Characterization of such size-induced effects and understanding the underlying fundamental mechanisms is especially important for the microelectronics and sensors industry where the critical dimension is rapidly approaching a few nanometers. The effect of miniaturization is especially intensive in the energy density (in the form of heat dissipation) in micro/nanoscale devices. This has catalyzed studies dealing with the application of thermal management at the nanoscale, especially on the measurement of thermal conductivity of nanoscale thin films [1]. More recently, the thermal conductivity of nanostructured materials have been analyzed in order to improve efficiency of newer energy conversion device technologies [2]. While classical concepts of thermal conductivity render it length-scale independent, there is growing evidence in the literature that the opposite is true [3, 4] at length scales comparable to the electron and phonon mean free path. Since bulk values can be extrapolated at the smaller scales, thermal characterization of nanoscale materials has been a very active area of research in the last decade [5, 6].

To measure thermal conductivity, one needs to determine the heat flux (typically set up by an energy source such as electrical heater) across the specimen in order to acquire the cross-plane thermal conductivity. Also the temperature drop between two separate points in the same plane is needed to be measured in order to obtain the in-plane thermal conductivity of the specimen. Two of the most common and well-established techniques for measuring *cross-plane* thermal conductivity of thin films and nanostructures are known as the 3ω and the steady-state [7] techniques. Other techniques, such as the membrane and bridge method, require the substrate to be removed thereby making the specimen freestanding [8, 9] and are commonly used for *in-plane* thermal conductivity measurement. For measurement of thermal properties of liquids, 3ω also can be utilized to realize thermal conductivity. In addition, the hot-wire technique is another method used to obtain thermal conductivity and thermal diffusivity of liquids [10].

The foundation of this paper lies on the 3ω technique, which uses electrical heating and electrical sensing-based measurements to set up the heat flux and for temperature measurement [11]. The conventional 3ω technique is very

H.-F. Lee · B. A. Samuel · M. A. Haque (✉)
Department of Mechanical and Nuclear Engineering,
The Pennsylvania State University, 317A Leonhard Building,
University Park, PA 16802, USA
e-mail: mah37@psu.edu

versatile as it allows for a variety of specimen configuration—line-heater-on-substrate, thin-film-on-substrate, and multilayered thin-film-on-substrate. In its simplest form, a metallic strip is deposited over the sample whose conductivity is to be measured, the metallic strip acts as the heating source and also as the sensing element [12, 13]. The strip metal film (acting both as a thermometer and a line heater) is driven by a periodically oscillating heat source (an a.c. current source) at a frequency of 'ω'. The heat dissipated in the line heater self heats itself and the underlying sample and caused temperature oscillations at '2ω' frequency. The temperature oscillations make the resistance of line heater vary at '2ω' frequency and consequently leading to voltage oscillations at '3ω' frequency. The thermal conductivity information of the underlying sample can be extracted from the amplitude of the 3ω voltage oscillations of the line heater. When the specimen is capable of self-heating (metals and semiconductors), it is usually made freestanding from the substrate so that the entire heat generated is exploited solely to set up a temperature gradient in the specimen and hence the measured thermal conductivity is unaffected by that of the substrate [14]. However, specimen on substrate configuration is actually a more accurate representation of real life applications as in microelectronic devices. Also, making the specimens freestanding requires additional processing steps and careful consideration on not affecting the specimen itself, which is generally difficult to execute on nanoscale specimens.

The motivation of the present study is therefore to relax the requirement of freestanding specimens and thus increase the versatility of the 3ω technique. We achieve this by developing an analytical model which accounts for the heat loss to the substrate so that the thermal conductivity of both the specimen and the substrate can be measured simultaneously. We demonstrate the new technique experimentally on both metallic (thin film aluminum) and semi-conducting (focused ion beam (FIB) deposited platinum) nanoscale specimens on substrates. It is important to note that FIB-deposited materials (especially Pt) have received increasing attention for use in nano-heaters, as nano-connectors for circuit repair, as protection layers, and in Transmission Electron Microscope specimen preparation applications. Their electrical properties are well characterized [15, 16], but the thermal properties are yet to be reported in the literature, which makes the new model and the experimental results useful for the FIB-deposited nanostructure applications.

Analytical model

We have developed a model that allows the 3ω technique to measure in-plane thermal conductivity of specimens that are not necessarily released from the substrate, as required by the conventional scheme. Figure 1 shows the conventional 3ω experimental setup, where an electrically conductive strip is connected to four electrodes. The two outer electrodes are used to apply a constant a.c. current in the strip, while the two inner electrodes are used to measure the third harmonic of the voltage $(V_{3\omega})$ across the strip. For insulating specimens (Fig. 1a), the substrate is the specimen and the top layer is the metal film that is used as heater and temperature sensor. This technique [12] measures only the cross-plane thermal conductivity (κ) by measuring the third harmonic voltage for two different frequencies f_1 and f_2, as given by the following equation.

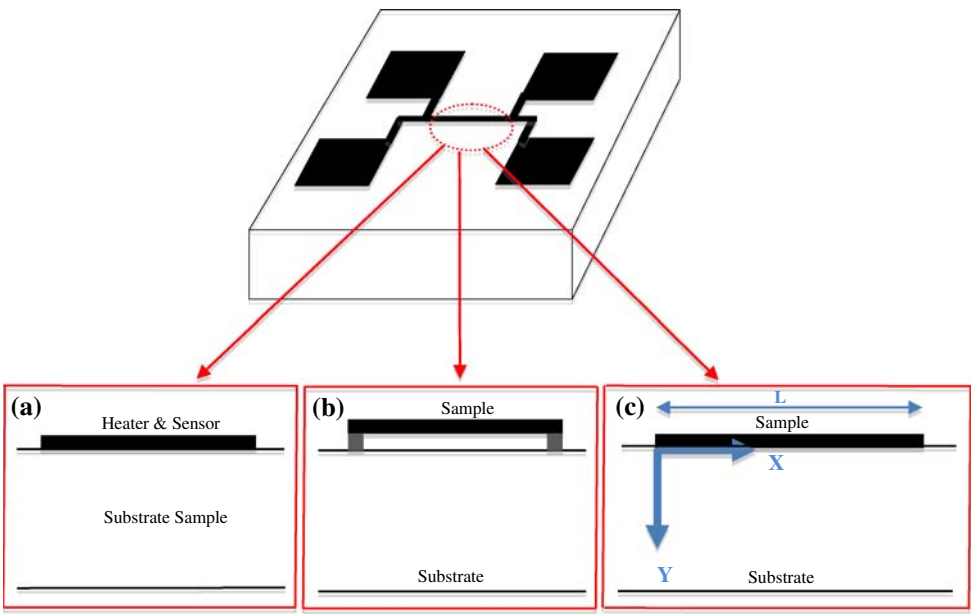

Fig. 1 The conventional 3ω setup for (**a**) electrically insulating materials, where the conducting layer acts as the heater and temperature sensor while the substrate itself is the specimen (**b**) electrically conducting and semiconducting specimens, released from the substrate to minimize heat losses to the substrate. (**c**) Setup for the new technique developed in this study obviates the additional step of releasing the specimen from the substrate

$$\kappa = \frac{V_{1\omega}^3 \ln\frac{f_2}{f_1}}{4\pi l R^2 (V_{3\omega,1} - V_{3\omega,2})} \frac{dR}{dT} \quad (1)$$

where $V_{1\omega}$ is the voltage across the metal strip at frequency ω, $V_{3\omega,1}$ and $V_{3\omega,2}$ are the voltages at the third harmonic for frequency f_1 and f_2 respectively, R and l are the metal line resistance and length respectively, and R′ is the slope of resistance as a function of temperature at the temperature of measurement. To measure the in-plane thermal conductivity, the specimen must be released from the substrate, and the experiments are conducted in vacuum to prevent heat losses. The in-plane thermal conductivity is obtained from the third harmonic voltage signal $(V_{3\omega})_w$ using the following expression [13],

$$V_{3\omega} \approx \frac{4I_0^3 \rho_e \rho_e'}{\pi^4 \kappa \sqrt{1 + (2\omega\gamma)^2}} \left(\frac{L}{S}\right)^3 \quad (2)$$

where I_0 and ω are the input current's amplitude and frequency respectively, ρ_e is the electrical resistivity of the specimen, ρ_e' is the thermal coefficient of resistance, L and S are the length and cross-sectional area of the specimen, and γ is the characteristic thermal time constant for the one-dimensional thermal transport process.

We present a model that accounts for the heat loss to the substrate by using a one-dimensional heat conduction equation with the heat source located on the nanostructure and considering the substrate as the heat sink. We assume that the temperature difference decays exponentially along y direction (as Fig. 1c, into the substrate) and is modeled as $\theta(x,t)e^{-\frac{y}{\lambda}}$. The parameter '$\lambda$' in the exponent relates to thermal wave penetration depth, which is equal to $\sqrt{\alpha_s/2\omega}$, where α_s is thermal diffusivity of substrate, ω is frequency of heat source and $\theta = T - T_0$ is the temperature change of substrate (T_0 is the initial temperature of substrate). The heat flux through the interface (y = 0) from the nanoscale metallic thin film to substrate is given by,

$$q_A|_{y=0} = \kappa_s A \left.\frac{\partial(\theta(x,y,t)e^{-\frac{y}{\lambda}})}{\partial y}\right|_{y=0} = \kappa_s A \left[-\frac{1}{\lambda}\theta(x,t)e^{-\frac{y}{\lambda}}\right]\Big|_{y=0} = -\frac{\kappa_s A \theta(x,t)}{\lambda} \quad (3)$$

We assume the temperature of the surface of substrate to be the same as temperature of the nanostructure directly above and in intimate contact with it, ignoring the interface resistance. Therefore, the temperature change of our sample along the longitudinal direction can be viewed as $\theta(x,t)$. The one dimensional heat conduction is then given by,

$$\rho C_p \frac{\partial\theta(x,t)}{\partial t} = \kappa \frac{\partial^2\theta(x,t)}{\partial x^2} + \frac{I_0^2 \sin^2\omega t}{LS}(R_0 + R'\theta(x,t)) - \frac{\kappa_s A}{LS\lambda}\theta(x,t) \quad (4)$$

where C_p and R_0 are the specimen specific heat and resistance at the reference temperature, R' is resistance derivative of temperature, κ_s is the substrate thermal conductivity and A is the area for heat transfer to the substrate. The boundary conditions and initial condition are as shown in Eq. 5.

$$\begin{cases} \theta(0,t) = 0 \\ \theta(L,t) = 0 \\ \theta(x,-\infty) = 0 \end{cases} \quad (5)$$

Solving Eq. 4 for θ, we obtain

$$\theta(x,t) = \sum_n \frac{D}{n\pi}[1 - (-1)^n] \sin\frac{n\pi x}{L} \frac{1}{G}\left[1 - \frac{\sin(2\omega t + \varphi)}{\sqrt{1 + \cot^2\varphi}}\right] \quad (6)$$

where, $D = \frac{I_0^2 R_0}{LS\rho C_p}$ and $G = \frac{n^2\pi\kappa}{\rho C_p L^2} + \frac{\kappa_s A}{\rho C_p LS\lambda}$

For the approximation: $n = 1$, we can write,

$$V(t) = \left(I_0 R + \frac{4I_0 R' D}{\pi^2 G}\right)\sin\omega t + \frac{2I_0 R' D}{\pi^2 G}\frac{1}{\sqrt{1 + 4\omega^2/G^2}}\cos(\omega t + \phi) + \frac{2I_0 R' D}{\pi^2 G}\frac{1}{\sqrt{1 + 4\omega^2/G^2}}\cos(3\omega t + \phi) \quad (7)$$

If $4\omega^2 \ll G^2 \Rightarrow 2\omega \ll \left(\frac{\kappa}{\rho C_p}\frac{\pi^2}{L^2} + \frac{1}{\rho C_p}\frac{\kappa_s A}{LS\lambda}\right)$, the magnitude of 3ω voltage becomes

$$V_{3\omega} \approx \frac{2I_0^3 R_0 R' L}{\pi^4 \kappa S + \frac{L\pi^2\kappa_s A}{\lambda}} \quad (8)$$

The average temperature change is then given by,

$$\bar{\theta} \approx \frac{4I_0^2 R_0 L}{\pi^4 \kappa S + \frac{L\pi^2\kappa_s A}{\lambda}} \quad (9)$$

Therefore, the thermal conductivity of wire can be derived from Eq. 8 as

$$\kappa \approx \frac{\left(\frac{2I_0^3 R_0 R' L}{V_{3\omega}} - \frac{L\pi^2\kappa_s A}{\lambda}\right)}{\pi^4 S} \quad (10)$$

We now have an analytical expression for the thermal conductivity of the nanoscale material, taking into consideration heat dissipation to the substrate as well. In the next section the accuracy of this model is verified experimentally.

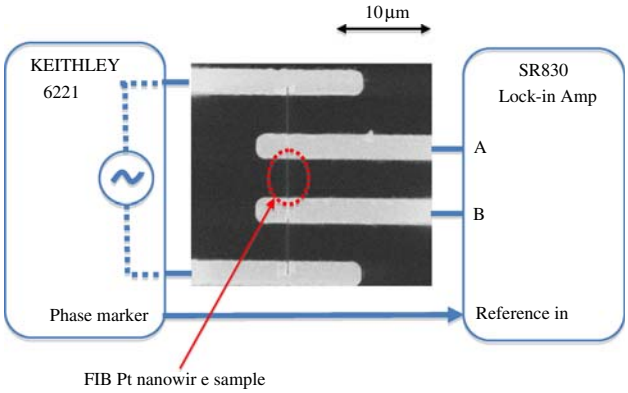

Fig. 2 Experimental setup for the 3ω technique applied on FIB-deposited Platinum

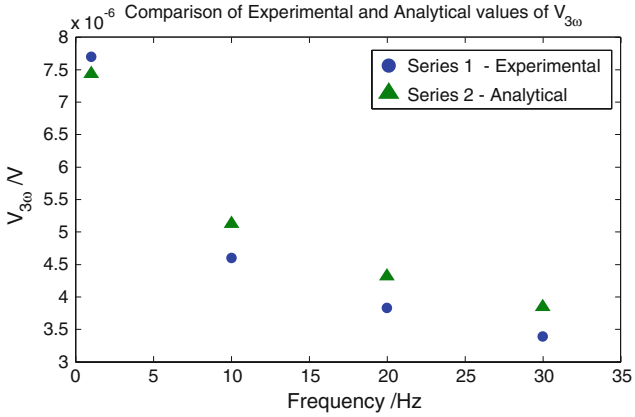

Fig. 3 The measured $V_{3\omega}$ and expected $V_{3\omega}$ of aluminum thin film

Experimental results and discussions

Figure 2 shows the experimental setup schematic along with a scanning electron micrograph of a focused-ion-beam deposited platinum nanowire across lithographically patterned gold electrodes. The substrate is a commercially available silicon wafer with about 500 nm thick thermally grown oxide layer at the top. The four-probe configuration of electrodes for measuring eliminates contact resistance and minimizes experimental error, for conducting nanowires the parasitic/contact resistances usually are of the same magnitude as the measured DUT (device-under-test) resistance. The experiments are performed in vacuum environment to prevent heat loss through convection. The main components of the experimental setup are the Keithley 6221 Constant Current Source and the Stanford SR830 Lock-in Amplifier. The constant current source passes a constant alternating current $I_0 \sin\omega t$ through the specimen, and the lock-in amplifier was used to measure 1ω and 3ω signals using differential input method. The key features of a 3ω experiment are the choice of amplitude of the ac current, the low frequency operating settings of the lock-in amplifier, and use of a high vacuum environment. From the analytical model we recognize a current limitation: $\frac{I_0^2 R' L\lambda}{n^2\pi^2\kappa\lambda S+\kappa_s LA} \ll 1$ implicit in the derivation of $\theta(x,t)$. Therefore, the amplitude of the applied current cannot be too large, but however from a measurement stand-point it has to be large enough so that the signal to noise ratio of the 3ω signal is satisfactory. The SR830 lock-in amplifier is proficient for measuring small a.c. signals which can reach nano-volt levels and has a very low level of noise floor. The most important parameter in using the lock-in amplifier is the time constant which decides the bandwidth of low pass filter, and we use $30 \sim 300$ s here for the frequency range of a.c. current from 30 to 1 Hz to fulfill the frequency limitation: $2\omega \ll \left(\frac{\kappa}{\rho C_p}\frac{\pi^2}{L^2} + \frac{1}{\rho C_p}\frac{\kappa_s A}{LS\lambda}\right)$.

The new model developed was first experimentally characterized and calibrated on a metal specimen of known thermal conductivity. The metal used is evaporated aluminum (lithographically patterned), lithographically patterned to be 100 μm long, 10 μm wide, and 130 nm thick. Figure 3, Series 1 presents the measured rms value of 3ω voltages in the frequency range $1 \sim 30$ Hz which matches well with the expected data, based on the analytical model, showing as Series 2. We observe that the 3ω voltages slightly increase with a decrease in the frequency. We fit this data to the Cahill's model, i.e. Eq. 1, to find out the thermal conductivity of glass substrate, resulting in a value of 1.07 W/mK at 297 K. By substituting this value of thermal conductivity for the glass substrate into our 3ω model, i.e. Eq. 10, we obtain the thermal conductivity of the aluminum thin film as shown in Fig. 4. Additionally, according to our model Eq. 8 implies a linear relationship between the 3ω voltage ($V_{3\omega}$) and the cube of the current amplitude (I_0^3), and this is experimentally verified and graphically shown in Fig. 5. Here we chose the value of 0.003 amp as the amplitude of a.c current in order to fulfill the current limitation criteria, previously mentioned.

After verifying the analytical model and calibrating the experimental setup, we performed experiments on FIB-deposited platinum nanowires. The specimen was 7 μm long, 600 nm wide, and 800 nm thick. Figures 6 and 7 individually show the $V_{3\omega}$ value and average temperature change measure experimentally from a setup, as shown in Fig. 2. The amplitude of a.c. current and the operating frequency we chose were 7.07 μA and $1000 \sim 400$ Hz, which satisfied the restrictions built into the analytical 3ω model. The value of thermal conductivity of FIB Platinum nanowire obtained from measurement is 40.97 W/mK at room temperature. For pure platinum, the thermal conductivity is 71.6 W/mK at room temperature. The variation seen is because the FIB-deposited Pt is not just purely Pt metal, but is a conducting metal-organic polymer

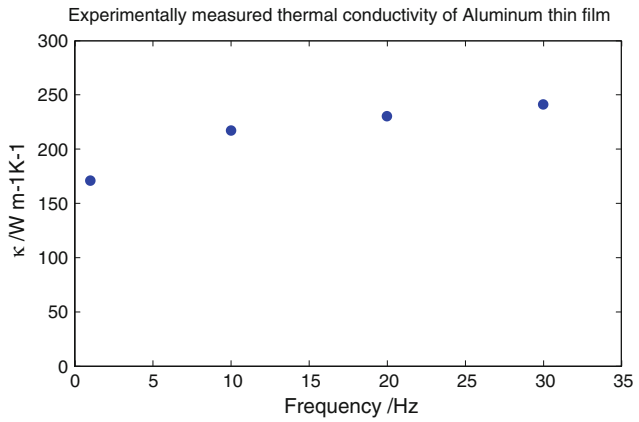

Fig. 4 Thermal conductivity of aluminum thin film

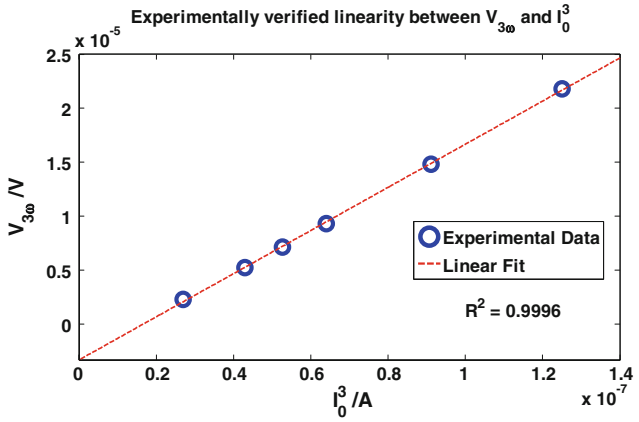

Fig. 5 The proportional relationship between $V_{3\omega}$ of aluminum thin film and I_0^3

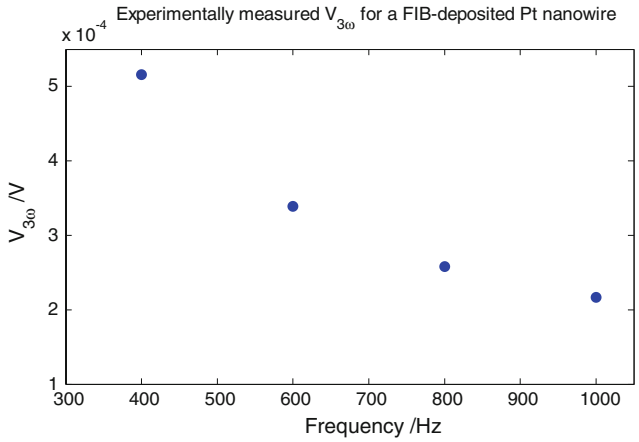

Fig. 6 The measured $V_{3\omega}$ for FIB-deposited Pt nanowire

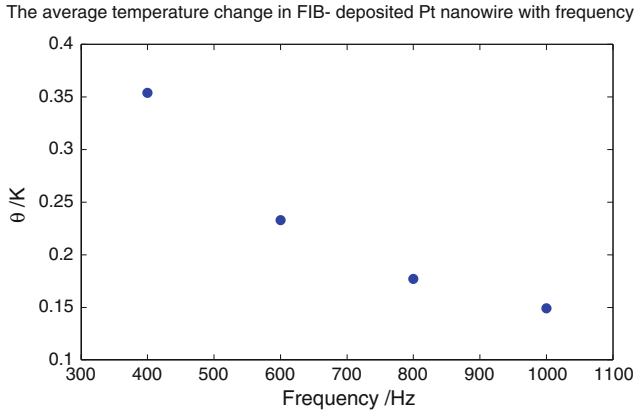

Fig. 7 The average temperature change of FIB Pt nanowire

($C_9H_{16}Pt$) which in its as-deposited form creates a nanostructure made of Pt and amorphous carbon mixture (The Ga^+ ion in the ion beam causes amorphization of the carbon). The thermal conductivity of amorphous carbon varies from 0.3 to 10 W/mK at room temperature. If we use a simple rule of mixtures like equation using 50% platinum contribution and 50% amorphous carbon contribution, we obtain an approximated thermal conductivity value of FIB-deposited platinum to be about 40.8 W/mK which matches our data very well. The measured value of thermal conductivity of FIB-deposited platinum nanowire is found to be in within the expected bounds. In addition, let's take a look at Eq. 8, the denominator of amplitude of $V_{3\omega}$ includes two terms, $\pi^4 \kappa S$ and $\frac{L\pi^2 \kappa_s A}{\lambda}$. In our case, the order of $\pi^4 \kappa S$ is 10^{-8}, and the order of $\frac{L\pi^2 \kappa_s A}{\lambda}$ is 10^{-11}. This means that$\pi^4 \kappa S$ is much larger than $\frac{L\pi^2 \kappa_s A}{\lambda}$, and thus $\frac{L\pi^2 \kappa_s A}{\lambda}$,which represents the heat loss from FIB platinum nanowire to substrate is very small in this case, and can be neglected, which concurs with one of the starting assumptions of the analytical model.

Conclusions

We have developed an analytical model extending the existing 3ω formulation to include characterizing nanostructures lying on substrate geometries. The biggest advantage of this technique is that it provides an easy and convenient way for characterization since it eliminates nanofabrication involved in making freestanding samples. It also allows simultaneous measurement of cross-plane thermal conductivity of the substrate and in-plane thermal conductivity of the nanostructured specimen. We have experimentally validated the model using aluminum thin films on glass substrates and FIB-deposited Pt nanowires on thermally grown silicon oxide. In addition we also present the first-ever thermal conductivity data for FIB-deposited Pt nanowires that are now extensively used as electrical interconnects/mechanical grips in MEMS/NEMS studies. The ease of specimen preparation, coupled with the ease of measurement and analysis make this technique a substantial improvement over the conventional 3ω method, especially for nanostructures.

Acknowledgements The authors gratefully acknowledge the Korea Institute of Metals and Machinery and the National Science Foundation, USA (ECS #0545683).

References

1. Cahill DG, Ford WK, Goodson KE, Mahan GD, Majumdar A, Maris HJ, et al. Nanoscale thermal transport. J Appl Phys. 2003;93(2):793–818.
2. Yoshino H, Papavassiliou G, Murata K. Low-dimensional organic conductors as thermoelectric materials. J Therm Anal Calorim. 2008;92(2):457–60.
3. Stewart D, Norris PM. Size effects on the thermal conductivity of thin metallic wires: microscale implications. Microscale Thermophys Eng. 2000;4(2):89–101.
4. Liang LH, Li BW. Size-dependent thermal conductivity of nanoscale semiconducting systems. Phys Rev B. 2006;73(15):4.
5. Sparavigna A. Lattice specific heat of carbon nanotubes. J Therm Anal Calorim. 2008;93(3):983–6.
6. Li D, Wu Y, Fan R, Yang P, Majumdar A. Thermal conductivity of Si/SiGe superlattice nanowires. Appl Phys Lett. 2003;83(15):3186–8.
7. Borca-Tasciuc T, Kumar AR, Chen G. Data reduction in 3 omega method for thin-film thermal conductivity determination. Rev Sci Instrum. 2001;72(4):2139–47.
8. Jansen E, Obermeier E. Thermal conductivity measurements on thin films based on micromechanical devices. J Micromech Microeng. 1996;6(1):118–21.
9. Shi L, Li D, Yu C, Jang W, Kim D, Yao Z, et al. Measuring thermal and thermoelectric properties of one-dimensional nanostructures using a microfabricated device. J Heat Transf. 2003; 125(5):881–8.
10. Tian F, Sun L, Venart J, Prasad R. Thermal conductivity and thermal diffusivity of poly(acrylic acid) by transient hot wire technique. J Therm Anal Calorim. 2009;96(1):67–71.
11. Borca-Tasciuc T, Chen G. Thermal conductivity: theory, properties and applications. New York: Kluwer Academic/Plenum Publishers, 2004.
12. Cahill DG, Katiyar M, Abelson JR. Thermal conductivity of a-Si:H thin films. Phys Rev B. 1994;50(9):6077.
13. Cahill DG. Thermal conductivity measurement from 30 to 750 K: the 3 omega method. Rev Sci Instrum. 1990;61(2):802–8.
14. Lu L, Yi W, Zhang DL. 3 omega method for specific heat and thermal conductivity measurements. Rev Sci Instrum. 2001;72(7):2996–3003.
15. Marzi GD, Iacopino D, Quinn AJ, Redmond G. Probing intrinsic transport properties of single metal nanowires: direct-write contact formation using a focused ion beam. J Appl Phys. 2004; 96(6):3458–62.
16. Langford RM, Wang TX, Ozkaya D. Reducing the resistivity of electron and ion beam assisted deposited Pt. Microelectron Eng. 2007;84(5–8):784–8.